Landslide susceptibility mapping along Bhalubang — Shiwapur area of mid-Western Nepal using frequency ratio and ...

Biswajeet Pradhan

Journal of Mountain Science

Landslide Susceptibility Mapping along Bhalubang – Shiwapur Area of Mid-Western Nepal Using Frequency Ratio and Conditional Probability Models

Amar Deep REGMI[1]*, Kohki YOSHIDA[2], Hamid Reza POURGHASEMI[3], Megh Raj DHITAL[4], Biswajeet PRADHAN[5]

1 Faculty of Technology, Nepal Academy of Science and Technology, Lalitpur-Khumaltar 44700, Nepal

2 Department of Geology, Faculty of Science, Shinshu University, Asahi 3-1-1, Matsumoto 3908621, Japan

3 College of Natural Resources & Marine Sciences, Tarbiat Modares University (TMU), Noor, 14115-335, Tehran, Iran

4 Central Department of Geology, Tribhuvan University, Kritipur 44613, Nepal

5 Faculty of Engineering, Department of Civil Engineering, Geosptial Information Science Research Centre (GISRC), University of Putra Malaysia, Serdang, Selangor Darul Ehsan 43400, Malaysia

*Corresponding author, e-mail: amardeep_regmi@yahoo.com; amardeep.regmi@gmail.com

Abstract: Roads constructed in fragile Siwaliks are prone to large number of instabilities. Bhalubang–Shiwapur section of Mahendra Highway lying in Western Nepal is one of them. To understand the landslide causative factor and to predict future occurrence of the landslides, landslide susceptibility mapping (LSM) of this region was carried out using frequency ratio (FR) and weights-of-evidence (W of E) models. These models are easy to apply and give good results. For this, landslide inventory map of the area was prepared based on the aerial photo interpretation, from previously published/unpublished reposts, and detailed field survey using GPS. About 332 landslides were identified and mapped, among which 226 (70%) were randomly selected for model training and the remaining 106 (30%) were used for validation purpose. A spatial database was constructed from topographic, geological, and land cover maps. The reclassified maps based on the weight values of frequency ratio and weights-of-evidence were applied to get final susceptibility maps. The resultant landslide susceptibility maps were verified and compared with the training data, as well as with the validation data. From the analysis, it is seen that both the models were equally capable of predicting landslide susceptibility of the region (W of E model (success rate = 83.39%, prediction rate = 79.59%); FR model (success rate = 83.31%, prediction rate = 78.58%)). In addition, it was observed that the distance from highway and lithology, followed by distance from drainage, slope curvature, and slope gradient played major role in the formation of landsides. The landslide susceptibility maps thus produced can serve as basic tools for planners and engineers to carry out further development works in this landslide prone area.

Keywords: Landslides; Frequency ratio; Weights-of-evidence; GIS; Himalaya

Introduction

Himalaya, the youngest and tectonically the most active mountain range of the world, was

formed as a result of the collision of Indian Plate and Eurasian Plate about 40 million years ago (Searle et al. 1987; Dewey et al. 1989). Nepal occupies the central portion of this 2400 km long Himalayan arc, extending for about 800 km in length. Together with flooding, landslides are the most severe types of natural hazards in Nepal, where the mountains occupy about 83% of the territory. Apart from causing loss of life and property, the landslides also seriously degrade the mountain environment and add an enormous sediment load to the streams and rivers. Large-scale deforestation, unplanned land use systems and the construction of physical infrastructure, such as roads, canals, and dams in the hazardous mountainous region, have contributed to landslides, debris flows, soil erosion, and floods (Rajbhandari et al. 2002).

The Mahendra Highway is a major highway in Nepal connecting East to West (Figure 1). Major portion of this highway runs through the plain Terai region and the Siwalik Hills. The part of the highway passing through these Siwaliks is mostly affected by severe landslide problem. The Bhalubang–Shiwapur section is one of the most severely affected parts of the Mahendra Highway where different types of slope failures are observed. This area is characterized by steeply dipping rocks consisting of sandstone, mudstone, and conglomerate (Tamrakar and Yokota 2008). In addition, differential weathering of rocks are observed along the highway and its surrounding areas. This portion of highway is often partially or fully blocked at different locations in every monsoon season because of the landslides. Understanding the types of landslides and preventing them from occurring through suitable land use planning and management are very
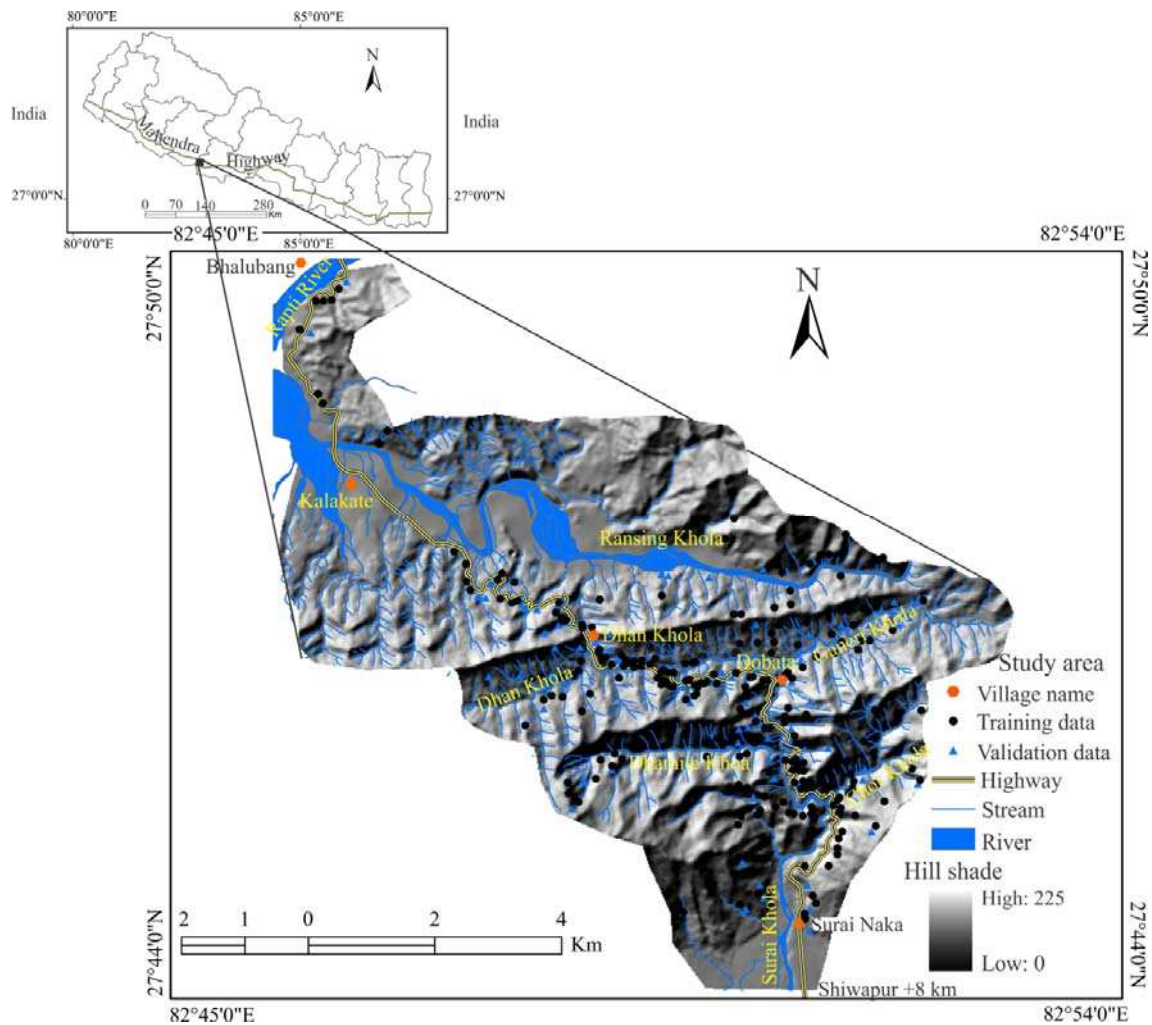

Figure 1 Study area with the distribution of landslides.

essential along the highway and its surrounding region. In landslide susceptibility mapping (LSM), landslide prone areas are determined by correlating some of the major factors that are responsible for the slope failure with the past distribution of landslides (Brabb 1984). LSM can be considered as a standard tool to understand effective land use management strategy that ultimately assist land management decision making process (Akgun 2012a). There are several approaches for developing landslide susceptibility and hazard map of a region (Varnes 1984; Jones 1992; Hutchinson 1992) and are categorized into three distinct groups: (i) deterministic (or engineering or geotechnical), (ii) the heuristic (or index) and (iii) the statistical methods (Clerici et al. 2006).

Deterministic approaches are mainly based on geotechnical and ground water properties of the rock and soil of unstable areas. In this case, specific mathematical models are used to find factor of safety of the unstable slopes (Gokceoglu and Aksoy 1996) and slope stability models are used to determine the landslide hazard (Clerici et al. 2014). As this approach requires large amount of input data for model building, it is suitable only when the ground conditions are fairly homogenous (Dai and Lee 2002).

The heuristic or index-based approach for landslide susceptibility mapping was first proposed by Anbalagan (1992). This approach is an indirect (or semi-direct), mostly qualitative, method that relies on the identification of instability factors responsible for the formation of the instabilities in that region. These instability factors are classified, ranked and weighted according to their assumed or expected importance in causing mass movements. Based on this information, heuristic and subjective decision rules are established to define possible unstable areas and the landslide susceptibility zones, respectively (Pachauri et al. 1998; Kayastha et al. 2013; Pellicani et. al. 2014). Recently, new decision support tools, comprising analytical hierarchy process (APH) (Komac 2006; Pourghasemi et al. 2012; Hasekiogullari and Ercanoglu 2013; Kayastha et al. 2013) and weighted linear combination models (Soeters and van Westen 1996: Guzzetti et al. 1999; Ayalew et al. 2004; Yoshimatsu and Abe 2006) are being used for LSM.

Statistical methods are the most commonly used approaches for LSM that involve statistical scrutiny between landslide distribution and the conditioning parameters that are influencing landslide occurrence so as to derive the association between topographical condition and landslide occurrence (Landslide risk assessment 2004). In this approach, relationship between distribution of past landslides and causative factor is observed by mapping the existing landslides, mapping or deriving a set of factors that are supposed to directly or indirectly influence the occurrences of the instabilities and to establish a statistical relationship between these factors and the instabilities (Fell et al. 2008). Among various statistical methods, bivariate (Dahal et al. 2008; Pourghasemi et al. 2011; Regmi et al. 2014; Jaafari et al. 2014; Demir et al. 2014; Shahabib et al. 2014; Ozdemir et al. 2013), and multivariate statistical methods are the most prominent ones. In literature, the most commonly used multivariate statistical methods are the discriminant analysis (Carrara et al. 2006; Santacana et al. 2003; Guzzetti et al. 2005, 2006; Baeza et al. 2010), the factor analysis (Ercanoglu and Gokceoglu 2002; Ercanoglu et al. 2004) and the logistic regression analysis (Ayalew and Yamagishi 2005; Akgun and Bulut 2007; Nefeslioglu et al. 2008; Yilmaz 2009; Bai et al. 2010; Pradhan and Lee 2010; Ercanoglu and Temiz 2011; Atkinson and Massari 2011; Devkota et al. 2013; Kavzoglu et al. 2013; Umar et al. 2014). Besides these, several researchers have used soft computing approaches for LSM, such as fuzzy logic (Ercanoglu and Gokceoglu 2002; Kanungo et al. 2006; Muthu et al. 2008; Pradhan and Lee 2009; Pradhan 2010; Pradhan 2011; Regmi et al. 2012; Zhu et al. 2014), artificial neural networks (Ermini et al. 2005; Kanungo et al. 2006; Melchiorre et al. 2008; Yilmaz 2009; Yilmaz 2010a; Pradhan and Lee 2010; Poudyal et al. 2010; Pradhan 2011; Zare et al. 2013; Bui et al. 2012b; Conforti et al. 2014), neuro fuzzy (Vahidnia et al. 2010; Sezer et al. 2011; Bui et al. 2012a; Pradhan 2012), support vector machine (Yao et al. 2008; Pradhan 2012; Bui et al. 2012c; Kavzoglu et al. 2013; Peng et al. 2014) and landslide inventory-based probabilistic methods (Lee and Pradhan 2007).

In the present work, LSM of the Bhalubang–Shiwapur section and its surrounding regions sufferings from instabilities   each year was

performed using statistical/probabilistic method referred to as FR model (Regmi et al. 2014; Jaafari et al. 2014; Demir et al. 2014; Shahabib et al. 2014; Ozdemir et al. 2013; Yalcin et al. 2011) and W of E model (Bonham-Carter 1991; Gokceoglu et al. 2005; Neuhäuser and Terhorst 2007; Dahal et at. 2008; Zhu and Wang 2009; Regmi et al. 2010a, b; Mohammady et al. 2012; Pourghasemi et al. 2013; Ozdemir et al. 2013; Regmi et al. 2014). It is very important to carry out the susceptibility mapping along the highway built within the Siwaliks as they are very prone to landsliding. Besides, several roads are being built in these fragile Siwaliks each year without giving due consideration to the general geology and morphology of the region. As most of the studies carried out so far are concentrated along the drainage basin and only few along the road section and very few on the roads constructed in the Siwaliks. Our study aims to fulfill this gap and tries to develop susceptible maps of the highways built in the fragile mountains like Siwaliks.

1   Study Area

The study area lies in Mid-Western Nepal and occupies parts of the Dang and Arghakhanchi districts. It is bounded by the latitudes 27°44'0" N and 27°50'0" N, and the longitudes 82°45'0" E and 82°53'30" E and extends for 70.77 km² (Figure 1). The East-West (or Mahendra) Highway passes through the central part of the study area (Figure 1). The main settlements in the study area are Bhalubang, Kalakate, Dobata, Dhan Khola and Shivgarhi. The altitude in the study area ranges from 170 m to 960 m and exhibits a very rugged topography with highly dissected gullies and steep slopes. Most of the mountain ridges in the study area are extending in the east–west direction, parallel to the main geological structures. The Rapti River is the major river system in the study area (Figure 1), while Ransing Khola and Surai Khola are its major tributaries. Dhan Khola is one of the tributaries of Ransing Khola, while Ganeri Khola and Dhamile Khola are the tributaries of Surai Khola. In the study area, the erosional landforms predominate over the depositional ones. Tropical to subtropical climatic condition prevails in the study area. The main characteristic of the

climate in the study area is the monsoon rainfall, which occurs between June and September and delivers an average of 85% of the total rainfall of the year (UN 1989).

2   Geological Setting

Tectonically, Nepal Himalaya can be subdivided into five major belts: Fore Himalaya, Higher Himalaya, Lesser Himalaya, Sub-Himalaya (Siwaliks) and the Indogangetic plane (Gansser 1964). These five belts are separated by major thrust faults, namely South Tibetan Detachment System (STDS), Main Central Thrust (MCT), Main Boundary Thrust (MBT) and Himalayan Frontal Thrust (HFT), which have created large amount of deformation in the rocks and soil, thus making them susceptible to landsliding (Regmi et al. 2014).

The Siwalik rocks of Middle Miocene to Pliocene crop out along the Bhalubang–Shiwapur highway section and its surrounding region (Figure 2).These rocks can be classified into five formations, namely, Bankas Formation, Chor Khola Formation, Suria Khola Formation, Dobata Formation, and the Dhan Khola Formation in the ascending order (Corvinus and Nanda 1994; Dhital et al. 1995). Red-purple mudstones, shales, and fine- to very fine-grained sandstones form the main lithology of the Bankas Formation. The Chor Khola Formation is divided into two members: Jungli Khola Member and Shivgarhi Member. The Jungli Khola Member is represented by fine- to medium-grained greenish grey sandstone interbedded with variegated mudstone, while the Shivgarhi Member is comprised of coarse-grained sandstone and grey mudstone with a few marl beds. Multi-storied, coarse to very coarse-grained 'salt and pepper' sandstones form the main lithology of the Surai Khola Formation. The beds yield a great amount of petrified wood in the form of stems, branches, and roots. The Dobata Formation is predominated by mudstones with minor amount of sandstones and conglomerates. The Dhan Khola Formation comprises compact and hard boulder- and pebble-bearing conglomerates with yellow mudstones in the lower part and loose conglomerates with yellow mudstones in the upper part (Dhital et al. 1995).

The main geological structure demarcating the study area is the Main Frontal Thrust (Dhital et al.
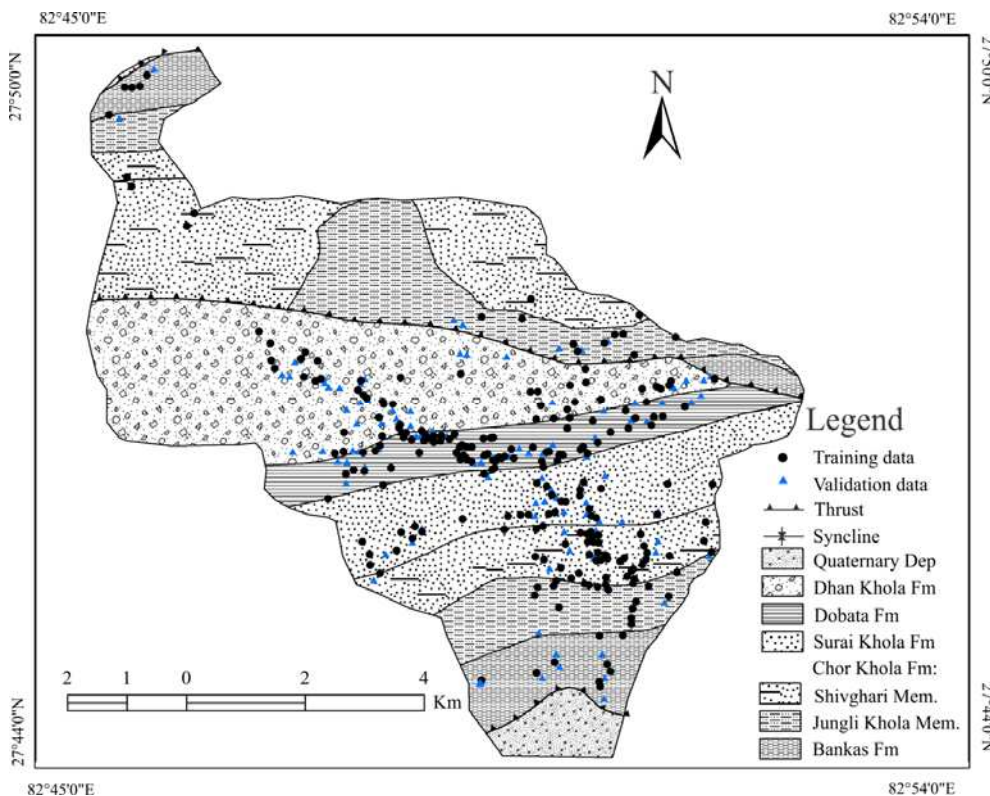
Figure 2 Geological map of the study area.

A total of 322 landslide locations were identified and mapped in the study area (Figure 1). Polygon map of landslides was prepared in the field, and they were converted to point data for the modeling purpose. Most of the landslides are located near the highway and river banks. In the case of geology, Dobata Formation contains more landslides, followed by Surai Khola and Dhan Khola Formation. All the landsides were mapped in 1:25,000 topographic map of the study area. The smallest landslide is about 0.048 m², while the largest landslide is about 0.061 km². Figure 3 shows the types of landslides observed in each geological formation.

1995). This thrust separates the Siwaliks from the Indogangetic plane lying to the south of it. Two other thrusts, namely Ransing Thrust and Sit Khola thrust pass through the central and northern part of the study area, respectively (Figure 2). One syncline lies in between the Ransing Thrust and Sit Khola Thrust (Figure 2).

3 Landslide Inventory

Acquiring information about past landslides is considered as the first and the most important step in landslide susceptibility study (Chacón et al. 2006) and is also considered as a fundamental part of the landslide hazard studies (Guzzetti et al. 1999; Ercanoglu and Gokceoglu 2004). Since landslide occurrences in the past and the present are keys to future spatial prediction (Guzzetti et al. 1999), a landslide inventory map is a prerequisite for such study. In this context, accurate detection of the location of landslides is very essential. We carried out a detailed field survey of the area after analyzing previously published and unpublished report from the study area, as well as aerial photographs and Google Earth images.

4 Spatial Database

The occurrence of landslides in any given area is dependent on a number of conditioning factors. Therefore it is important to identify and analyze the factors leading to landslides to develop LSM (Lee and Oh 2011). For GIS based LSM, it is important to construct a digitized database. Hence, the data preparation in this step involved the digitization or creation of a GIS database. LSM also requires identification of a suitable set of instability factors. In this respect, twelve factors are considered for susceptibility analysis including slope gradient, slope aspect, plan curvature, altitude, stream power index (SPI), topographic wetness index (TWI), sediment transport index (STI), lithology, distance from faults, land use, distance from rivers, and distance from highway.

As most of the landslides are located near the highway and along the banks of the river, these two conditioning factors are considered. Besides, geology of the region is also the major controlling factor in the landslide formation along the highway section. Topography and land use are other controlling factors for the instabilities in this region, hence they are considered. Topographic maps and aerial photographs provided by the Department of Survey, Government of Nepal (GoN) were used as the basic data sources for generating various thematic layers using ArcGIS 9.3, ILWIS 3.8 and

Figure 3 Types of landslides observed in each lithological unit. (a) Landslide related to difference in litho-type observed in Bankas Formation, near Bhalubang; (b) Huge landslide observed in Jungali Khola Member of Chor Khola Formation in Ransing Khola; (c) Landslide observed at Shivgarhi Member of Chor Khola Formation, near Chor Khola; (d) Landslide observed in Surai Khola Formation, near the bridge of Surai Khola; (e) Large landslide observed in Dobata Formation, at Ganeri Khola, near Dobata; (f) Instability observed in the conglomerates of Dhan Khola Formation, near Dhan Khola.

ArcView 3.3 software.

4.1 Digital Elevation Model (DEM) and its derivatives

Digitized contour map and spot height map provided by the Department of Survey, GoN were used in creating digital elevation model (DEM) of the study area. A pixel size of 20 m×20 m was selected in the present study. From the DEM, slope gradient, slope aspect, plan curvature, altitude, stream power index (SPI), topographic witness index (TWI), and sediment transport index (STI) maps were obtained using Arc GIS 9.3 and SAGA GIS.

The slope gradient map was produced from the DEM using spatial analysis tool of Arc GIS (Fig. 4a). Increase in the slope gradient cause increase in the shear stress in soil or in other unconsolidated material, making it susceptible to failure; hence it is considered as one of the most important factors causing slope instability (Oh and Lee 2011). The steeper the slope, the greater is the landslide probability. The slope in the study area varies from 0° to 53.11° and is reclassified into five classes (Figure 4a).

The horizontal direction to which a mountain slope faces is referred to as the slope aspect. Most of the south facing slopes of the Himalayan terrain are either barren or are poorly vegetated. In addition, these slopes receive more orographic rainfall than other slopes. Hence, rapid mass movements occur on these south facing slopes (Chauhan et al. 2010). The slope aspect map was produced from the DEM and was divided into nine classes in the present study (Figure 4b).

Altitude is another important parameter that is frequently used for landslide susceptibility studies (Juang et al. 1992; Pachauri and Pant 1992; Çevik and Topal 2003). Landslides are generally associated with higher elevation (Pachauri and Pant 1992; Ercanoglu et al. 2004). In the present study area, the altitude ranges from 173m to 961 m and is reclassified into six classes with an interval of 150 m (Figure 4c).

The plan curvature values represent the morphology of the topography (Lee and Min 2001; Erener and Duzgun 2010). Mathematically, it is defined as the reciprocal of the radius of a circle that is tangent to a point on a curve (Roberts 2001).

The curvature analysis allows dividing the area into concave, convex, and flat surfaces (Figure 4d) and consequently may help to identify zones that exhibit proneness to landslide (Manciniet al. 2010).

Stream power index (SPI), topographic witness index (TWI), and sediment transport index (STI) are the other conditioning factors derived from DEM in SAGA GIS. The erosive power of overland flow is measured by the SPI. It is also considered as one of the main factors underwriting toward stability of the area. The SPI is given by the following equation (Moore and Grayson 1991):

$$SPI = A_s \tan \beta \qquad (1)$$

where A_s and β represent the specific catchment area and local slope gradient measured in degrees, respectively. In the present study, SPI is divided into 5 classes (Figure 4e).

The soil moisture and surface saturation is indicated by the topographic wetness index (TWI) as it can quantify the control of local topography on hydrological process. It is given by,

$$TWI = \ln\left(\frac{a}{\tan \beta}\right) \qquad (2)$$

Here, a = specific cumulative upslope area draining through a point (per unit contour length), and $\tan\beta$ = local slope angle of the specific grid, which is used to replace approximately the local hydraulic gradient under steady state conditions. In this study, TWI is divided into 5 classes (Figure 4f).

Erosional and depositional process of a stream is characterized by the sediment transport index (STI). Mathematically, it can be written as,

$$STI = (A_s/22.13)^{0.6} \times (sin \ \beta/0.0896)^{1.3} \qquad (3)$$

where A_s and β are the upstream area and slope at a given cell, respectively. In the present study, STI is divided into 5 classes (Figure 4g).

4.2 Geological factors

Lithology and major geological structures that demarcate the study area are discussed in this section.

Lithology is considered as one of the major parameters known to influence landslides in some regions as certain geological conditions are considered to quicken weathering process, thus preparing the rock for sliding (Goretti 2010; Regmi et al. 2013). There are abundant associations
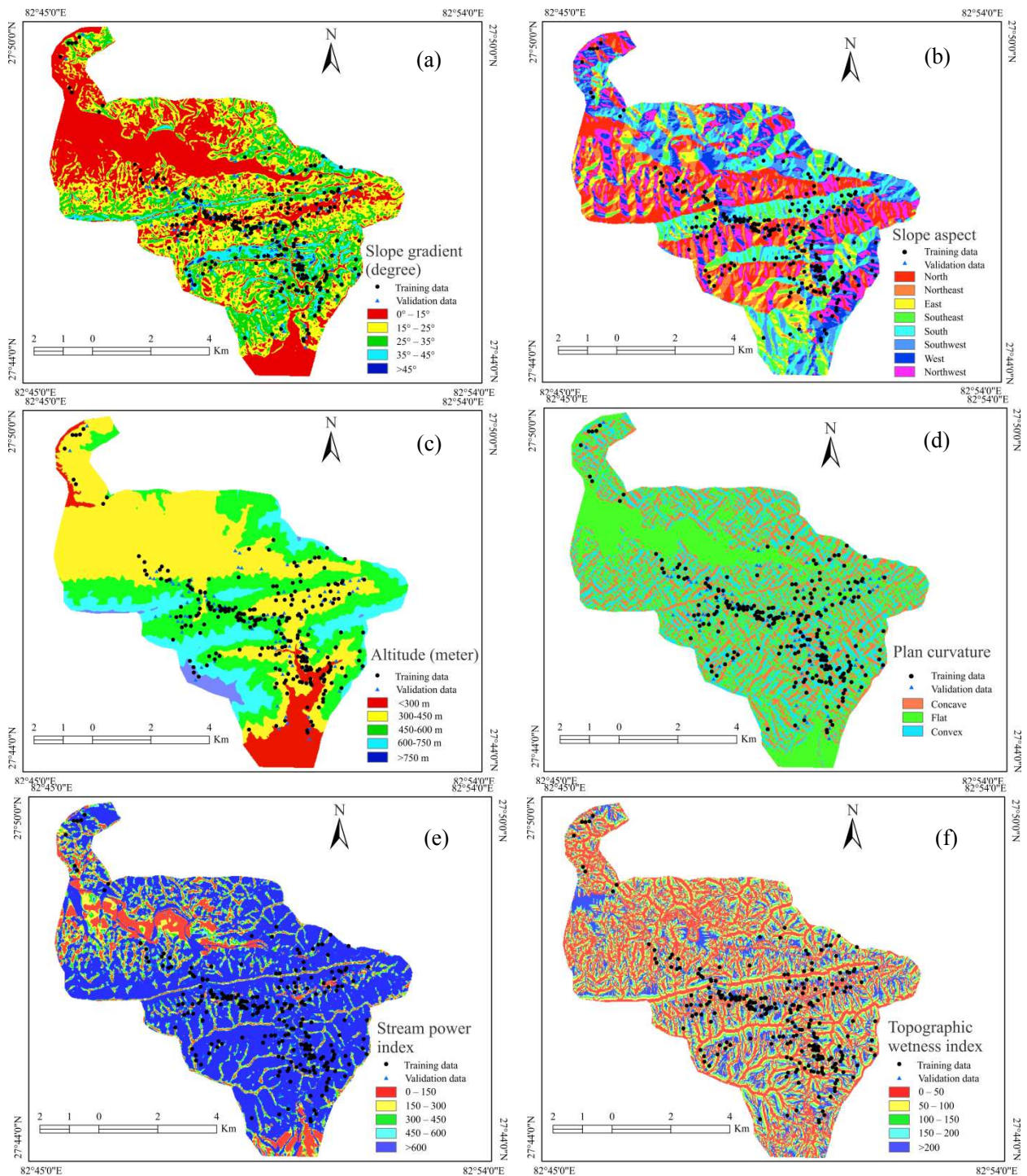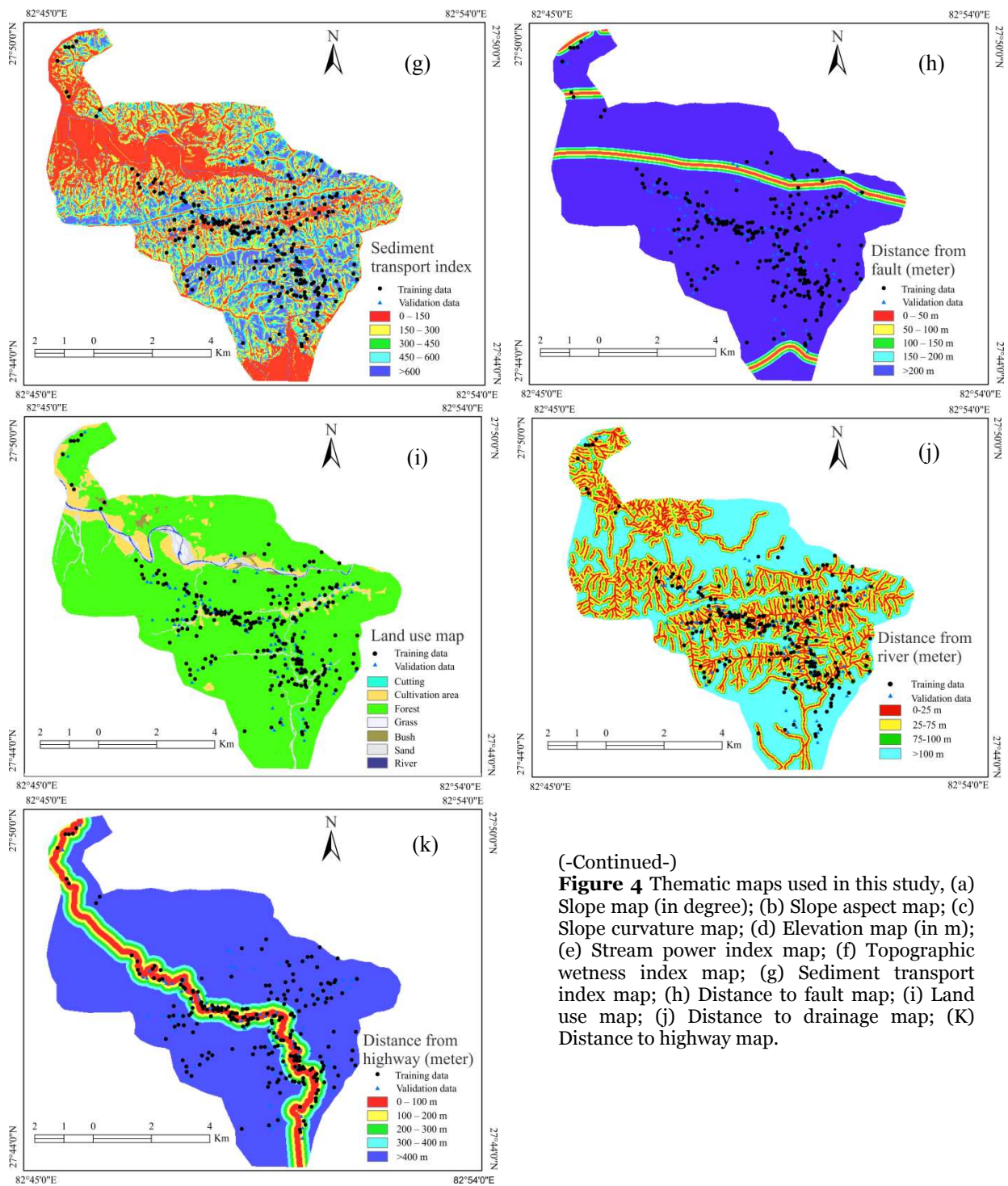
Figure 4 Thematic maps used in this study, (a) Slope map (in degree); (b) Slope aspect map; (c) Slope curvature map; (d) Elevation map (in m); (e) Stream power index map; (f) Topographic wetness index map; (g) Sediment transport index map; (h) Distance to fault map; (i) Land use map; (j) Distance to drainage map; (K) Distance to highway map. (-To be continued-)

between the particular rock type and the associated mass movement phenomena indicating the importance of lithology on landslide formation (Sidle et al. 1985). Mudstone, sandstone, and conglomerate are the main rock types in the study area. The lithological map was produced by the help of previous geological map developed by Dhital et al. (1995) and from detailed field

(-Continued-)
Figure 4 Thematic maps used in this study, (a) Slope map (in degree); (b) Slope aspect map; (c) Slope curvature map; (d) Elevation map (in m); (e) Stream power index map; (f) Topographic wetness index map; (g) Sediment transport index map; (h) Distance to fault map; (i) Land use map; (j) Distance to drainage map; (K) Distance to highway map.

investigation (Figure 2).

The strength of rock is reduced as a result of the presence of tectonic structures (fault), as these tectonic structures break the rock mass, reducing its strength and making it susceptible to failure (Donati and Turrini 2002). Fault distance map was created by buffering it with a buffer zone of 100 m

interval (Figure 4h). The fault lines were derived from the geological map (Figure 2).

4.3 Land use map

A land use map is used to identify the land use classes such as forest, agricultural land, settlement area, as well as other earth surface features such as

roads, manufacturing plants, and harbors and it helps us to understand the stability of a slope. The land covered by forest regulates water flow and water infiltration regularly, whereas the cultivated land affects the slope stability owing to saturation of covered soil (Devkota et al. 2013). A land use map, with seven classes of land use, provided by the Department of Survey, GoN was adopted in our study. As shown in Figure 4i our study area consists of more than 87.66% forest, 6.6% agriculture land, 4% sand, and others occupy a minor portion.

4.4 Distance from river map

Occurrence of landslides in the study area is found to be frequent along the river banks. Therefore, distance from river was considered as another geomorphology related causative factor for instabilities. Subsequently, a distance from river map was generated as the streams disrupt the stability of slopes either by toe undercutting or by saturating the parts of the materials lying within the water level of the stream ways (Gökçeoglu and Aksoy 1996; Çevik and Topal 2003; Yalçin 2007, 2008). The distance from river map is developed from the vector map of rivers by buffering and rasterizing in ArcGIS 9.3 software. The resultant map is then divided into 5 classes (Figure 4j).

4.5 Distance from highway map

As natural condition of a slope is damaged during the road construction process, road construction activity is also considered one of the controlling factors for the stability of slopes. In addition, the road construction causes the loss of load both in topography and slope buttress. Besides these, road cut exposes the joints and fractures making the rocks susceptible to failure. The distance to highway map was created from the road network map obtained from the Department of Survey of GoN by buffering it in ArcGIS 9.3 with a buffer distance of 100 m (Figure 4k).

5 Methodology

Among various statistical approaches of LSM, we have adopted frequency ratio and weights of evidence models for the present study. Details of each approach are described in the following subsections.

5.1 FR model

The FR model is relatively a simple and understandable probabilistic model, in which the FR is defined as the ratio of area where landslides occurred to the total study area. It is also the ratio of probability of a landslide occurrence to a non-occurrence for a given attribute (Bonham-Carter 1994; Pradhan and Lee2009; Lee and Pradhan 2006, 2009).This model is based on the observed relationship between each factor and distribution of landslides. The frequency ratio can be expressed as,

$$FR = \frac{\dfrac{Npix(SX_i)}{\sum_{i=1}^{m} SX_i}}{\dfrac{Npix(X_j)}{\sum_{j=1}^{n} Npix(X_j)}} \qquad (4)$$

where $Npix(SX_i)$ is the number of pixels with landslides within class i of parameter variable X, $Npix(X_j)$ is the number of pixels within parameter variable X_j, m is the number of classes in the parameter variable X_i, and N is the number of parameters in the study area (Regmi et al. 2014). The landslide susceptibility index can be generated by the summation of each factor's Fr value as:

$$LSI = \sum FR \qquad (5)$$

If the ratio is greater than 1, the greater is the relationship between a landslide occurrence and the specific factor's attribute; and if it is less than 1, the opposite is true.

5.2 Wof E model

The second model used in the present study is WofE model. This model uses log-linear form of Bayesian probability model to estimate the relative importance of evidence by statistical means. Recently, W of E model has been extensively used in landslide susceptibility mapping (Neuhäuser and Terhorst 2007; Regmi et al. 2010a, b; van Westen et al. 2003; Sharma and Kumar 2008; Dahal et al. 2008; Pourghasemi et al. 2013; Ozdemir et al. 2013; Regmi et al. 2014).

The $WofE$ model is fundamentally based on the calculation of positive and negative

weights W^+ and W^-. A detailed description of the mathematical formulation of the method is available in Bonham-Carter (1994, 1989). The method calculates the weight for each landslide predictive factor (A) based on the presence or absence of landslides (B) within the area, (Bonham-Carter et al. 1994) as follows:

$$W_i^+ = ln\frac{P\{B|A\}}{P\{B|\bar{A}\}} \qquad (6)$$

$$W_i^- = ln\frac{P\{\bar{B}/A\}}{P\{\bar{B}/\bar{A}\}} \qquad (7)$$

$$Weight\ contrast\ (C) = W^+ + W^- \qquad (8)$$

$$S^2W^+ = \frac{1}{N\{B \cap A\}} + \frac{1}{B \cap \bar{A}} \qquad (9)$$

$$S^2W^- = \frac{1}{\{\bar{B} \cap A\}} + \frac{1}{\{\bar{B} \cap \bar{A}\}} \qquad (10)$$

$$S(C) = \sqrt{S^2W^+ + S^2W^-} \qquad (11)$$

where P is the probability and ln is the natural log. Similarly, B is the presence of potential landslide predictive factor, $\bar{B}$ is the absence of a potential landslide predictive factor, A is the presence of landslide and $\bar{A}$ is the absence of a landslide (Regmi et al. 2014). A positive weight (W^+) indicates that the predictable variable is present at the landslide locations and the magnitude of this weight is an indication of the positive correlation between the presence of the predictable variable and the landslides. A negative weight (W^-) indicates the absence of predictable variable and shows the level of negative correlation (Dahal et al. 2008). The overall spatial association between the relevant factors and events is reflected by C (Lee et al. 2012). The S^2W^+ and S^2W^- are the variances of positive and negative weights, respectively. The studentized value of C, calculated as the ratio of C to its standard deviation, C/S(C), serves as a guide to the significance of the spatial association (Lee et al. 2012).

6   Results and Discussion

In the present study, we have used two models, (i) the frequency ratio model, and (ii) the W of E model to derive the relationships between the landslide distribution and the landslide conditioning factors. From the analysis, we can get the following results:

6.1 Landslide susceptibility based on the frequency ratio model

Frequency ratio model is very easy to implement and can be used to determine the level of correlation between landslide locations and landslide conditioning factors. This model is built on the basis of the observed relationship between landslide locations and the conditioning factors (Table 1). The final landslide susceptibility map obtained by the FR model is shown in Figure 5.

The relationship between slope angle and landslide shows that the greater the slope angle, the larger is the number of landslides (Table 1). In addition, it is seen that slope class > 45° has the highest value of FR, while 0–15° slope class has the least value. All other slope classes have FR > 1, indicating positive correlation between landslides and slope angle. Increase in slope angle results in the increase in shear stress of the material constituting the slope (especially soil and other unconsolidated material), thus making them susceptible to sliding. Hence, gentle slopes are expected to be less susceptible to sliding (Regmi et al. 2014). In the case of slope aspect, NE, S, SW and W facing slopes are having FR value >1 (Table 1), showing positive correlations with the landslide. Human intervention in the south, south west, west and NE-facing slopes is higher than the slopes facing in other directions. Beside this, river under-cutting takes places along these slopes, thus making them more prone to landsliding. In the case of curvature, FR is highest for convex slope (1.41), followed by concave slope (1.29), while this value is less than 1 for flat slopes (Table 1). Concave slopes can hold more water during the rainfall event and they can retain that water for long time. This retained water can lead to the formation of landslides in such slopes. On the other hand, convex slopes are regularly attacked by the external forces. Due to which constant expansion and contraction takes place in the slopes, thus making them susceptible to sliding (Lee and Pradhan 2006). In the case of altitude, FR value higher than 1 is found at the altitude ranging from 300–600 m. FR is less than 1 for both the higher and lower lying area, i.e. FR<1 for <300 m and for >600 m altitude STI indicating high landslide susceptibility. However, FR value decreases as the value of TWI increases. In the case of STI, FR is greater than 1

Factor	Class	A	$\bar{A}$	B	$\bar{B}$	FR = A/B	$\bar{A}/\bar{B}$	W^+	W^-	C	S^2W^+	S^2W^-	S(C)	C/S(C)
Slope degree	0°–15°	2.59	97.41	37.25	62.75	0.07	1.55	−2.67	0.44	−3.11	0.17	0	0.41	−7.51
	15°–25°	45.26	54.74	33.17	66.83	1.36	0.82	0.31	−0.2	0.51	0.01	0.01	0.13	3.87
	25°–35°	35.78	64.22	22.84	77.16	1.57	0.83	0.45	−0.18	0.63	0.01	0.01	0.14	4.61
	35°–45°	14.22	85.78	6.3	93.7	2.26	0.92	0.81	−0.09	0.9	0.03	0.01	0.19	4.8
	>45°	2.16	97.84	0.44	99.56	4.85	0.98	1.58	−0.02	1.6	0.2	0	0.45	3.52
Aspect	North	12.93	87.07	18.28	81.72	0.71	1.07	−0.35	0.06	−0.41	0.03	0	0.2	−2.09
	North East	15.52	84.48	11.55	88.45	1.34	0.96	0.3	−0.05	0.34	0.03	0.01	0.18	1.88
	East	7.33	92.67	8.13	91.87	0.9	1.01	−0.1	0.01	−0.11	0.06	0	0.25	−0.45
	South East	6.47	93.53	10.91	89.09	0.59	1.05	−0.52	0.05	−0.57	0.07	0	0.27	−2.14
	South	18.53	81.47	13.86	86.14	1.34	0.95	0.29	−0.06	0.35	0.02	0.01	0.17	2.05
	South West	13.36	86.64	10.79	89.21	1.24	0.97	0.21	−0.03	0.24	0.03	0	0.19	1.26
	West	10.78	89.22	10.58	89.42	1.02	1	0.02	0	0.02	0.04	0	0.21	0.1
	North West	15.09	84.91	15.9	84.1	0.95	1.01	−0.05	0.01	−0.06	0.03	0.01	0.18	−0.34
Plan curvature (100/m)	Concave	31.03	68.97	25.61	74.39	1.21	0.93	0.19	−0.08	0.27	0.01	0.01	0.14	1.89
	Flat	31.47	68.53	49.21	50.79	0.64	1.35	−0.45	0.3	−0.75	0.01	0.01	0.14	−5.28
	Convex	37.5	62.5	25.18	74.82	1.49	0.84	0.4	−0.18	0.58	0.01	0.01	0.14	4.26
Altitude (meter)	<300 m	3.45	96.55	7.54	92.46	0.46	1.04	−0.78	0.04	−0.83	0.13	0	0.36	−2.3
	300 m–450 m	50.43	49.57	45.81	54.19	1.1	0.91	0.1	−0.09	0.19	0.01	0.01	0.13	1.41
	450 m–600 m	41.81	58.19	31.15	68.85	1.34	0.85	0.29	−0.17	0.46	0.01	0.01	0.13	3.47
	600 m–750 m	3.02	96.98	13.64	86.36	0.22	1.12	−1.51	0.12	−1.62	0.14	0	0.38	−4.23
	>750 m	1.29	98.71	1.86	98.14	0.7	1.01	−0.36	0.01	−0.37	0.33	0	0.58	−0.63
SPI	<300	0.86	99.14	11	89	0.08	1.11	−2.55	0.11	−2.65	0.5	0	0.71	−3.74
	300–600	2.59	97.41	8.26	91.74	0.31	1.06	−1.16	0.06	−1.22	0.17	0	0.41	−2.95
	600–900	6.9	93.1	7.52	92.48	0.92	1.01	−0.09	0.01	−0.09	0.06	0	0.26	−0.36
	900–1200	12.07	87.93	6.94	93.06	1.74	0.94	0.55	−0.06	0.61	0.04	0	0.2	3.02
	>1200	77.59	22.41	66.28	33.72	1.17	0.66	0.16	−0.41	0.57	0.01	0.02	0.16	3.59
TWI	<5	79.31	20.69	59.16	40.84	1.34	0.51	0.29	−0.68	0.97	0.01	0.02	0.16	6
	5–7	16.81	83.19	23.77	76.23	0.71	1.09	−0.35	0.09	−0.43	0.03	0.01	0.18	−2.47
	7–11	3.88	96.12	12.26	87.74	0.32	1.1	−1.15	0.09	−1.24	0.11	0	0.34	−3.65
	11–16	0	100	3.46	96.54	0	1.04	0	0.04	0	0	0	0	0
	>16	0	100	1.34	98.66	0	1.01	0	0.01	0	0	0	0	0
STI	<68	9.48	90.52	33.17	66.83	0.29	1.35	−1.25	0.3	−1.56	0.05	0	0.22	−6.94
	68–181	29.31	70.69	21.16	78.84	1.39	0.9	0.33	−0.11	0.44	0.01	0.01	0.14	3.01
	181–349	16.81	83.19	15.97	84.03	1.05	0.99	0.05	−0.01	0.06	0.03	0.01	0.18	0.35
	181–637	16.81	83.19	10.62	89.38	1.58	0.93	0.46	−0.07	0.53	0.03	0.01	0.18	3.02
	>637	27.59	72.41	19.09	80.91	1.45	0.89	0.37	−0.11	0.48	0.02	0.01	0.15	3.26

Table 1 Spatial relationship between each factor and landslide by the FR, and Wo E models Surai Khola area, Nepal (-To be continued-)

(-continued-)

Table 1 Spatial relationship between each factor and landslide by the FR, and Wo E models Surai Khola area, Nepal

Factor	Class	A	$\bar{A}$	B	$\bar{B}$	$FR = A/B$	$\bar{A}/\bar{B}$	W^+	W^-	C	S^2W^+	S^2W^-	S(C)	C/S(C)
Geology	Bankas Fm	6.03	93.97	8.16	91.84	0.74	1.02	−0.3	0.02	−0.33	0.07	0	0.28	−1.18
	Jangali Khola Mem	10.78	89.22	17	83	0.63	1.07	−0.46	0.07	−0.53	0.04	0	0.21	−2.49
	Sivgarhi Mem	20.69	79.31	24.41	75.59	0.85	1.05	−0.17	0.05	−0.21	0.02	0.01	0.16	−1.32
	Surai Khola Fm	14.66	85.34	12.96	87.04	1.13	0.98	0.12	−0.02	0.14	0.03	0.01	0.19	0.77
	Dobata Fm	28.02	71.98	8.46	91.54	3.31	0.79	1.2	−0.24	1.44	0.02	0.01	0.15	9.82
	Dhan Khola Fm	19.83	80.17	26.35	73.65	0.75	1.09	−0.28	0.08	−0.37	0.02	0.01	0.16	−2.24
	Quaternary Deposit	0	100	2.65	97.35	0	1.03	0	0.03	0	0	0	0	0
Distance from Faults (meter)	0 m−50 m	0.86	99.14	2.5	97.5	0.34	1.02	−1.07	0.02	−1.08	0.5	0	0.71	−1.53
	50 m−100 m	0	100	2.46	97.54	0	1.03	0	0.02	0	0	0	0	0
	100 m−150 m	1.72	98.28	2.46	97.54	0.7	1.01	−0.35	0.01	−0.36	0.25	0	0.5	−0.72
	150 m−200 m	0.43	99.57	2.46	97.54	0.18	1.02	−1.74	0.02	−1.76	1	0	1	−1.76
	>200 m	96.98	3.02	90.12	9.88	1.08	0.31	0.07	−1.19	1.26	0	0.14	0.38	3.28
Land use	Cutting	0.86	99.14	0.11	99.89	8.11	0.99	2.09	−0.01	2.1	0.51	0	0.71	2.94
	Cultivation	2.59	97.41	6.6	93.4	0.39	1.04	−0.94	0.04	−0.98	0.17	0	0.41	−2.37
	Forest	96.12	3.88	87.67	12.33	1.1	0.31	0.09	−1.16	1.25	0	0.11	0.34	3.67
	Grass	0	100	0.36	99.64	0	1	0	0	0	0	0	0	0
	Bush	0.43	99.57	0.58	99.42	0.75	1	−0.29	0	−0.29	1	0	0	−0.29
	Sand	0	100	4.06	95.94	0	1.04	0	0.04	0	0	0	0	0
	River	0	100	0.63	99.37	0	1.01	0	0.01	0	0	0	0	0
Distance from River (meter)	0 m−25 m	14.66	85.34	18.51	81.49	0.79	1.05	−0.23	0.05	−0.28	0.03	0.01	0.19	−1.51
	50 m−75 m	39.22	60.78	31.22	68.78	1.26	0.88	0.23	−0.12	0.35	0.01	0.01	0.13	2.62
	75 m−100 m	28.02	71.98	10.48	89.52	2.67	0.8	0.98	−0.22	1.2	0.02	0.01	0.15	8.21
	>100 m	18.1	81.9	39.79	60.21	0.45	1.36	−0.79	0.31	−1.1	0.02	0.01	0.17	−6.42
Distance from Highway (meter)	0 m−100 m	28.88	71.12	6.31	93.69	4.57	0.76	1.52	−0.28	1.8	0.02	0.01	0.15	12.37
	100 m−200 m	15.95	84.05	5.7	94.3	2.8	0.89	1.03	−0.12	1.14	0.03	0.01	0.18	6.36
	200 m−300 m	40.95	59.05	5.25	94.75	7.8	0.62	2.05	−0.47	2.53	0.01	0.01	0.13	18.86
	300 m−400 m	6.03	93.97	5	95	1.21	0.99	0.19	−0.01	0.2	0.07	0	0.28	0.72
	>400 m	8.19	91.81	77.73	22.27	0.11	4.12	−2.25	1.42	−3.67	0.05	0	0.24	−15.31

for STI value in between 50–150, indicating higher level of correlation with landslides (Table 1). For the lithology, it can be seen that Dobata Formation contains the highest value of FR (3.13) indicating very high correlation with landsides, followed by Surai Khola Formation (1.13) (Table 1). All the other formations show lower correlation with the landslides as they have <1 values of FR (Table 1). Faults have very little influence in the landslide formation as most of the landslides are located far (>200 m) from the faults. In the case of land use, cutting area shows the highest correlation with the landslide formation (FR = 8.11). However, the cutting area occupies very little area in the study area. Most part of the study area is covered by forest and this class of land use also shows positive correlation with the landslides (FR = 1.1). All other land use classes show negative correlation with the landslide formation (FR <1) (Table 1). In the case of distance from river, the distance in between 0 and 25 m shows the highest correlation with the landslides. The highway has a major influence in the formation of landslides in the

Figure 5 Susceptibility map from frequency ratio model.
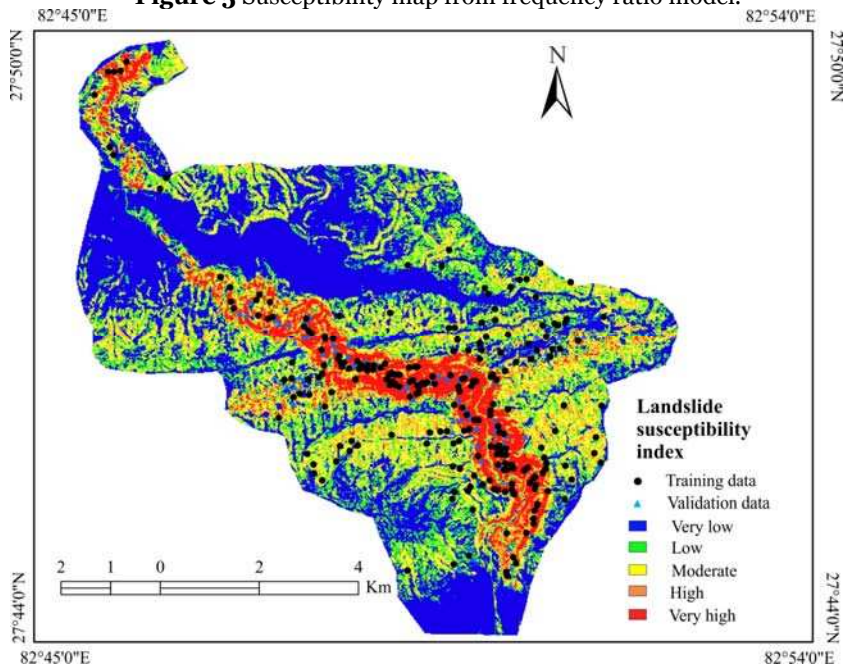
Figure 6 Susceptibility weights of evidence model.

study area, as most of the landslides are located very close to the highway. The distance between 0–400 m shows the maximum correlation with the landslides in the study area (for 0–100 m, FR = 4.57, 100–200 = 2.8, 200–300 = 7.8, 300–400 = 1.21), while the distance >400 m shows very little correlation with the landslide formation (FR = 0.11) (Table 1).
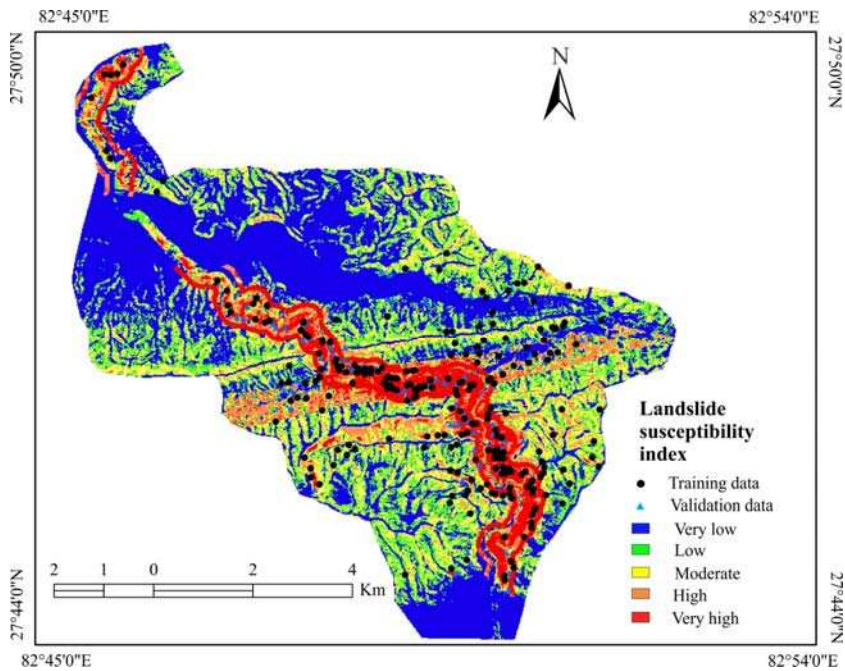
6.2 Landslide susceptibility based on W of E model

The W of E method was used to derive and calculate the spatial association values such as W^+ and W^- and C between the landslide distribution and the landslide conditioning factors. C is positive for a positive spatial association and

negative for a negative spatial association. The studentized value of C, the ratio of C to standard deviation or C/S(C), serves as a guide to the significance of spatial association and acts as a measure of relative certainty of the posterior probability (Bonham-Carter 1991). The relationship between landslides and the landslide conditioning factors, contrast, and studentized C are presented in Table 1. The C/S(C) values derived based on W of E model were assigned to the classes of each thematic layers to produce multiclass weighted maps for all evidence, which were overlaid in order to calculate a LSI map (Figure 6).

Based on the value of C/S(C), it can be seen that this value is highest for slope gradient >45°. However, this value is positive for the slope >25°, indicating higher susceptibility with reference to landslides in the study area. In case of slope aspect, NE, S, SW and W trending slopes have higher C/S(C) values indicating higher correlation with the landslides. Among these, NE, S and SW trending slopes have C/S(C)>1, while W trending slope has C/S(C) value 0.1 (Table 1). The convex slope has the highest value of C/S(C) (4.26), followed by concave slope (1.89) (Table 1), indicating high landslide susceptibility in these slopes, while flat slopes have negative C/S(C). In the case of altitude, the range in between 300 m and 600 m has highest C/S(C) value, indicating high landslide susceptibility at this range of elevation. Higher C/S(C) values are noted for higher SPI values, indicating higher susceptibility to landslides. Higher C/S(C) values are observed at lower TWI class, i.e. 0–5 class of TWI has C/S(C) value of 6 (Table 1), indicating higher susceptibility to landslides. Among different lithological classes, Dobata Formation has the highest C/S(C) value, followed by Surai Khola Formation. These lithological units show maximum susceptibility with reference to landslides in the study area. Faults in the study area play very little role in the formation of landslides; hence C/S(C) value is very small for different classes of fault distance (Table 1). Cutting and forest covered land show maximum susceptibility to landslides as they have positive C/S(C). The distance from river parameter also has shown positive influence towards slope destabilization as seen from the C/S(C) values. Slope saturation might be the reason for this phenomenon. Distances in between 50–100 m

have very high C/S(C) value. Several landslides are located at the uphill side as well as the downhill side of the highway that passes through the center of the study area. Maximum landslides are located within the distance of 300 m from the highway as indicated by the C/S(C) value. This may be due to the unplanned road construction activity in the study area.

6.3 Landslide susceptibility verification and comparison

The overall performance of the analysis is generally judged on the number of correctly classified cells, and so a validation process is required (Regmi et al. 2014). The landslide susceptibility maps of the study area were verified by comparing the existing landslide data and landslide susceptibility analysis results (Chung and Fabbri 1999). Success rate curves were prepared from the training data (226 (70%)) that were used for model building process and prediction rate curves were formed with the validation data (106 (30%)) (Figure 1, 2). The area under the curve (AUC) was calculated from 100 subdivisions of LSI values of all cells in the study area and the cumulative percentage of landslide occurrences in the classes. The AUC was obtained for both the training and the validation data (Figure 7). The result showed both FR and Wof E models show similar performances, with the W of E model being a better one (success rate, 83.39%;prediction rate, 79.59 %) than FR model (success rate, 83.31%; prediction rate, 78.58%) (Figures 7a and 7b). Besides, the various susceptible zones occupied in both the models were compared (Figure 8). From the figure, it is seen that the areas occupied by various susceptible zones for both the models are similar.

In Nepal, many roads have been constructed in the fragile Siwaliks without giving due consideration to the morphology of the area. Proper mitigation measures are not applied for instabilities during the road construction period, and hence these roads suffer from large number of instabilities each year. Huge amount of money is spent in restoring the conditions of these roads. Besides, new roads are being constructed throughout the country in the fragile Siwalik Hills without paying any attention to the general geology

and the instabilities that may occur and can cause large havoc in future. Instead of constructing large number of roads, few roads that are stable and are free from instabilities should be constructed. In

Figure 7 (a) Success rate curve for frequency ratio model (83.31) and weights of evidence model (83.39) (b) Prediction rate curve for frequency ratio model (AUC = 78.58) and weights of evidence model (79.59).

Figure 8 Area occupied by various susceptible zones in FR model and WoE model.

this respect, more studies are needed from different parts of the country to evaluate the road construction practices and their positive and negative impacts on people as well as on the environment.

7   Conclusions

The newly constructed roads in the fragile Siwaliks suffer from a large number of mass movement phenomena each year. They are serious threats to life and property damage. Landslide susceptibility mapping can be one of the preliminary steps towards understanding the possible causes of landslides and in minimizing these damages. In this respect, landslide susceptibility mapping of the Bhalubang–Shiwapur road section and its surrounding region was preformed based on widely accepted statistical models, such as frequency ratio and weights of evidence models with the aid of GIS. Slope gradient, slope aspect, slope curvature, elevation, SPI, TWI, SPI, STI, lithology, distance from faults, land use, distance from river, and distance from highway were used as the main conditioning factors for landslide susceptibility of the region. Based on literature review, aerial photo interpretation and multiple field visits, landslide inventory map of the region was prepared. Out of these 332 landslides, 70% (226) were randomly selected for model building purpose and the remaining 30% (106) of the landslides were used for validation purpose. From the analysis, distance to highway was considered to be the leading factor in the formation of instabilities in the region; the second most important factors were the distance to river and lithology respectively. As the highway passes through the banks of rivers, both the river and the highway act mutually in creating several landslides in the region. Besides this, the lithology consists of competent sandstone and very loose mudstone in most places. This contrast in lithology is also the cause of several instabilities in the region. Further,
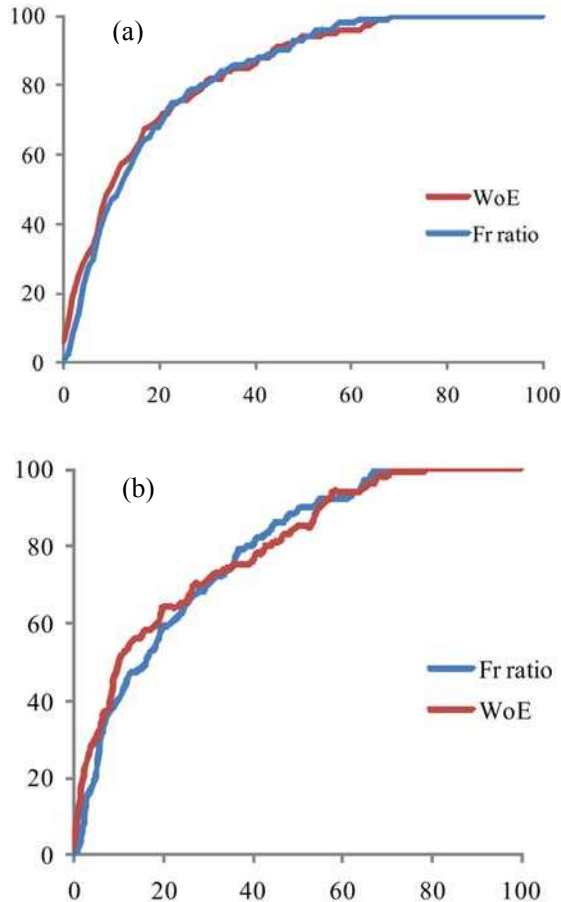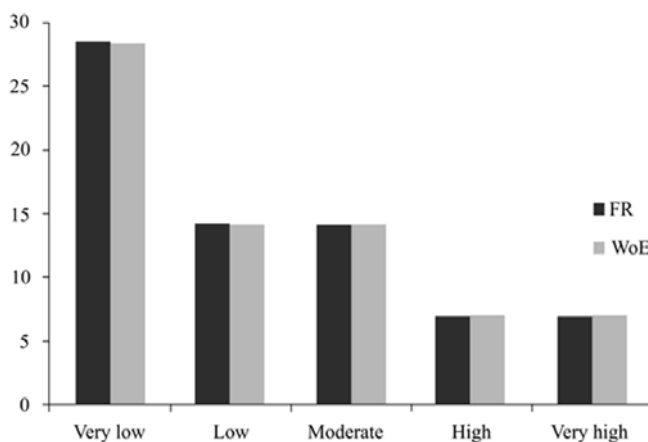
conglomerate is highly jointed and fractured, creating a good environment for the formation of instabilities. Beside these, slope aspect, slope angle, slope curvature, SPI, TWI, STI, and land use have some impact in the landside susceptibility of the region, while faults are not favorable for the landslide formation in this area. The performances of both these models were verified by both the success rate curve and prediction rate curve. From the analysis, it is seen that both the models were very effective in predicting the landslide susceptibility of the region (W of E model (success rate = 83.39, prediction rate = 79.59); FR model (success rate = 83.31, prediction rate = 78.58)). These landslide susceptibility maps can be used as a planning tool by prioritizing areas for controlling the landslide effects. Using these maps, planners can decide where to make development projects and where not to. Besides, proper mitigating measures can be applied in high susceptible zones if some projects are to be created.

Acknowledgement

References

Akgun A (2012a) A comparison of landslide susceptibility maps produced by logistic regression, multi-criteria decision, and likelihood ratio methods: a case study at İzmir, Turkey. Landslides 9 (1): 93-106. DOI: 10.1007/S10346-011-0283-7

Akgun A, Sezer EA, Nefeslioglu HA, et al. (2012b) An easy-to-use MATLAB program (MamLand) for the assessment of landslide susceptibility using a Mamdani fuzzy algorithm. Computers & Geosciences 38(1):23–34. DOI: 10.1016/j.cageo.2011.04.012

Akgun A, Bulut F (2007) GIS-based landslide susceptibility for Arsin-Yomra (Trabzon, North Turkey) region. Environmental Geology 51: 1377-1387. DOI: 10.1007/s00254-006-0435-6

Atkinson PM, Massari R (2011) Auto logistic modelling of susceptibility to landsliding in the Central Apennines, Italy. Geomorphology 130(1–2): 55-64. DOI: 10.1016/j.geomorph.2011.02.001

Anbalagan R (1992) Landslide hazard evaluation and zonation map- ping in mountainous terrain. Engineering Geology 32: 269-277. DOI: 10.1016/0013-7952(92)90053-2

Ayalew L, Yamagishi H, Ugawa N (2004) Landslide susceptibility mapping using GIS based weighted linear combination, the casein Tsugawa area of Agano River, Niigata Prefecture, Japan. Landslides 1(1): 73-81. DOI: 10.1007/s10346-003-0006-9

Ayalew L and Yamagishi H (2005) The application of GIS-based logistic regression for landslide susceptibility mapping in the Kakuda–Yahiko Mountains, Central Japan. Geomorphology 65(2): 15-31. DOI: 10.1016/j.geomorph.2004.06.010

Baeza C, Lantada N, Moya J (2010) Influence of sample and terrain unit on landslide susceptibility assessment at La Pobla de Lillet, Eastern Pyrenees, Spain. Environmental Earth Sciences 60: 155-167.

Bai SB, Wang J, Lü G, et al. (2010) GIS-based logistic regression for landslide susceptibility mapping of the Zhongxian segment in the Three Gorges area, China. Geomorphology 115: 23-31.

Bonham-Carter GF, Agterberg FP, Wright DF (1989) Weights of evidence modelling: a new approach to mapping mineral potential, in Agterberg FP, Bonham-Carter GF, (Eds.), Statistical Applications in the Earth Sciences: Geological Survey Canada Paper 89-9, pp 171-183.

Bonham-Carter GF (1991) Integration of geoscientific data using GIS. In: Good child MF, Rhind DW, Maguire DJ (Eds.) Geographic Information Systems: Principle and Applications. Longman, London, UK. pp 171-184.

Bonham-Carter GF (1994) Geographic information systems for geoscientists: modeling with GIS. In: Bonham-Carter F (Ed.) Computer Methods in the Geosciences. Pergamon, Oxford, UK. p. 398.

Brabb EE (1984) Innovative approaches to landslide hazard and risk mapping. Proceed. IV Int. Symp. Landslides, Toronto, 1, 307–324.

Bui DT, Pradhan B, Lofman O, et al. (2012a) Landslide susceptibility mapping at Hoa Binh province (Vietnam) using an adaptive neuro-fuzzy inference system and GIS. Computers & Geosciences 45: 199-211. DOI: 10.1016/j.cageo.2011.10.031

Bui DT, Pradhan B, Lofman O, et al. (2012b) Landslide susceptibility assessment in the Hoa Binh province of Vietnam: a comparison of the Levenberg-Marquardt and Bayesian regularized neural networks. Geomorphology 171–172: 12–29. DOI: 10.1016/j.geomorph.2012.04.023

Bui DT, Pradhan B, Lofman O, et al. (2012c) Landslide susceptibility assessment in Vietnam using support vector machines, decision tree and Naïve Bayes models. Mathematical Problems in Engineering 2012, Article ID: 974638. DOI: 10.1155/2012/974638

Carrara A, Cardinali M, Detti R, et al. (2006). GIS techniques and statistical models in evaluating landslide hazard. Earth Surface Processes and Landforms 16(5): 427-445. DOI: 10.1002/esp.3290160505

Çevik E, Topal T (2003) GIS-based landslide susceptibility mapping for a problematic segment of the natural gas pipeline, Hendek (Turkey). Environmental Geology 44(8): 949-962. DOI: 10.1007/s00254-003-0838-6

Chacon J, Irigaray C, Fernandez T, et al. (2006) Engineering

geology maps: landslides and geographical information systems. Bulletin of Engineering Geology and the Environment 65: 341-411. DOI: 10.1007/s10064-006-0064-z

Chauhan S, Sharma M, Arora MK (2010) Landslide susceptibility zonation of the Chamoli Region, Garhwal Himalayas, using Logistic Regression Model. Landslides 7(4): 411–423. DOI: 10.1007/s10346-010-0202-3

Chung CJ, Fabbri AG (1999) Probabilistic prediction models for landslide hazard mapping. Photogrammetric Engineering & Remote Sensing 65(12): 1389-1399.

Clerici A, Perego S, Tellini C, et al. (2006) A GIS-based automated procedure for landslide susceptibility mapping by the conditional analysis method: the Baganza valley case study (Italian Northern Apennines). Environmental Geology 50: 941-961.

Conforti M, Pascale S, Robustelli G, et al. (2014) Evaluation of prediction capability of the artificial neural networks for mapping landslide susceptibility in the Turbolo River catchment (northern Calabria, Italy). Catena 113: 236-250. DOI: 10.1007/s00254-006-0264-7

Corvinus G, Nanda AC (1994) Stratigraphy and palaeontology of the Siwalik Group of Surai Khola and Rato Khola in Nepal. Neues Jahrbuch fuer Geologie und Palaeontologie Abhandlungen. Marz; 1911: 25-68.

Dahal RK, Hasegawa S, Nonomura A, et al. (2008) GIS-based weights-of-evidence modeling of rainfall-induced landslides in small catchments for landslide susceptibility mapping. Environmental Geology 54(2): 314-324. DOI: 10.1007/s00254-007-0818-3

Dai FC, Lee CF (2002) Landslide characteristics and slope instability modelling using GIS, Lantau Island, Hong Kong. Geomorphology 42: 213-228. DOI: 10.1016/S0169-555X(01)00087-3

Devkota KC, Regmi AD, Pourghasemi HR, et al. (2013) Landslide susceptibility mapping using certainty factor, index of entropy and logistic regression models in GIS and their comparison at Mugling–Narayanghat road section in Nepal Himalaya. Natural Hazards (65): 1-31. DOI: 10.1007/s11069-012-0347-6

Demir G, Aytekin M, Akgun A (2014) Landslide susceptibility mapping by frequency ratio and logistic regression methods: an example from Niksar–Resadiye (Tokat, Turkey). Arabian Journal of Geosciences. DOI 10.1007/s12517-014-1332-z

Dewey JF, Cande S, Pitman III WC (1989) Tectonic evolution of the Indian/Eurasia Collision Zone. Ecolgae Geologicae Helvetiae, 82(3): 717-734. Key: citeulike:224505

Dhital MR, Gajural AP, Pathak D, et al. (1995) Geology and structure of the Siwaliks and Lesser Himlaya in the Surai Khola-Bardanda area, Mid-Western Nepal. Bulletin of the Department of Geology, Tribhuvan University. Kathmandu, Nepal. 4: 1-70.

Donati L, Turrini MC (2002) An objective method to rank the importance of the factors predisposing to landslides with the GIS methodology: application to an area of the Apennines (Valnerina; Perugia, Italy). An objective method to rank the importance of the factors predisposing to landslides with the GIS methodology: application to an area of the Apennines (Valnerina; Perugia, Italy) 63(3-4): 277-289. DOI: 10.1016/S0013-7952(01)00087-4

Ercanoglu M, Temiz FA (2011) Application of logistic regression and fuzzy operators to landslide susceptibility assessment in Azdavay (Kastamonu, Turkey). Environmental Earth Sciences 64(4): 949-964. DOI: 10.1007/s12665-011-0912-4

Ercanoglu M, Gokceoglu C (2002) Assessment of landslide susceptibility for a landslide prone area (north of Yenice, NW Turkey) by fuzzy approach. Environmental Geology 41: 720-730.

Ercanoglu M, Gokceoglu C (2004) Use of fuzzy relations to produce landslide susceptibility map of a landslide prone area (West Black Sea Region, Turkey). Engineering Geology 75: 229-250. DOI: 10.1016/j.enggeo.2004.06.001

Ercanoglu M, Gokceoglu C, van Asch TWJ (2004) Landslide susceptibility zoning north of Yenice (NW Turkey) by multivariate statistical techniques. Natural Hazards 32(1): 1-23. DOI: 10.1023/B:NHAZ.0000026786.85589.4a

Erener A, Düzgün HSB (2010) Improvement of statistical landslide susceptibility mapping by using spatial and global regression methods in the case of More and Romsdal (Norway). Landslides 7(1): 55-68. DOI: 10.1007/s10346-009-0188-x

Ermini L, Catani F, Casagli N (2005) Artificial neural networks applied to landslide susceptibility assessment. Geomorphology 66: 327-343. DOI: 10.1016/j.geomorph.2004.09.025

Fell R, Corominas J, Bonnard C, et al. (2008) Guidelines for landslide susceptibility, hazard and risk zoning for land use planning. Engineering Geology 102: 99-111. DOI: 10.1016/j.enggeo.2008.03.014

Ganser A (1964) Geology of the Himalaya. Inter Science John Wiley, London, UK.

Gokceoglu C, Aksoy H (1996) Landslide susceptibility mapping of the slopes in the residual soils of the Mengen region (Turkey) by deterministic stability analyses and image processing techniques. Landslide susceptibility mapping of the slopes in the residual soils of the Mengen region (Turkey) by deterministic stability analyses and image processing techniques 44: 147-161. DOI:10.1016/S0013-7952(97)81260-4

Gokceoglu C, Sonmez H, Nefeslioglu HA, et al. (2005) The 17 March 2005 Kuzulu landslide (Sivas, Turkey) and landslide-susceptibility map of its near vicinity. Engineering Geology 81: 65-83. DOI: 10.1016/j.enggeo.2005.07.011

Goretti KKM (2010) Landslide occurrence in the hilly areas of Bududa Districts in Eastern Uganda and their causes. Unpublished PhD thesis, Makerere University, Uganda. p. 106.

Gorsevski PV, Jankowski P (2010) An optimized solution of multi-criteria evaluation analysis of landslide susceptibility using fuzzy sets and Kalman filter. Computers & Geosciences 36: 1005-1020. DOI: 10.1016/j.cageo.2010.03.001

Guzzetti F, Carrara A, Cardinali M, et al. (1999) Landslide hazard evaluation: a review of current techniques and their application in a multi-scale study, Central Italy. Geomorphology 31: 181-216. DOI: 10.1016/S0169-555X(99)00078-1

Guzzetti F, Reinchenbach P, Cardinali M, et al. (2005) Probabilistic landslide hazard assessment at the basin scale. Geomorphology 72: 272-299. DOI: 10.1016/j.geomorph.2005.06.002

Guzzetti F, Reichenbach P, Ardizzone F, et al. (2006) Estimating the quality of landslide susceptibility models. Geomorphology 81: 166-184. DOI: 10.1016/j.geomorph.2006.04.007

Hasekiogullari GD, Ercanoglu M (2012) A new approach to use AHP in landslide susceptibility mapping: a case study at Yenice (Karabuk, NW Turkey). Natural Hazards 63(2): 1157-1179. DOI: 10.1007/s11069-012-0218-1

Hutchinson JN (1992) Landslide Hazard Assessment. Proceedings of the 6th International Symposium on Landslides, Christchurch, New Zealand. 3: 3-35.

Jaafari A, Najafi A, Pourghasemi HR, et al. (2014) GIS-based frequency ratio and index of entropy models for landslide susceptibility assessment in the Caspian forest, northern Iran. International Journal of Environmental Science and Technology 11(4): 909-926. DOI:10.1007/s13762-013-0464-0

Juang CH, Lee DH, Sheu C (1992). Mapping slope failure potential using fuzzy sets. Journal of Geotechnical Engineering, 118(3): 475-494. DOI: 10.1061/(ASCE)0733-9410(1992)118:3(475)

Kayastha P, Dhital MR, Smedt F De (2013) Application of the analytical hierarchy process (AHP) for landslide susceptibility mapping: A case study from the Tinau watershed, west Nepal. Computers and Geosciences, 52:398–408. DOI: 10.1016/j.cageo.2012.11.003

Kanungo DP, Arora MK, Sarkar S, et al. (2006) A comparative study of conventional, ANN black box, fuzzy and combined

neural and fuzzy weighting procedures for landslide susceptibility zonation in Darjeeling Himalayas. Engineering Geology 85: 347-366. DOI: 10.1016/j.enggeo.2006.03.004

Komac M (2006) A landslide susceptibility model using the analytical hierarchy process method and multivariate statistics in Perialpine Slovenia. Geomorphology 71: 17-28. DOI: 10.1016/j.geomorph.2005.07.005

Lee EM, Jones DKC (2004) Landslide risk assessment. Thomas Telford, London, UK. p 454.

Lee S, Pradhan B (2006) Probabilistic landslide hazards and risk mapping on Penang Island, Malaysia. Journal of Earth System Science 115(6): 661-672. DOI: 10.1007/s12040-006-0004-0

Lee S, Kim YS, Oh HJ (2012) Application of a weights-of-evidence method and GIS to regional groundwater productivity potential mapping. Journal of Environmental Management 96: 91-105. DOI:10.1016/j.jenvman.2011.09.016

Lee S, Min K (2001) Statistical analyses of landslide susceptibility at Yongin, Korea. Environmental Geology 40: 1095-1113. DOI: 10.1007/s002540100310

Lee S, Pradhan B (2007) Landslide hazard mapping at Selangor, Malaysia using frequency ratio and logistic regression models. Landslides 4: 33-41. DOI: 10.1007/s10346-006-0047-y

Mancini F, Ceppi C, Ritrovato G (2010) GIS and statistical analysis for landslide susceptibility mapping in the Daunia area, Italy. Natural Hazards & Earth System Sciences 10: 1851-1864. DOI: 10.5194/nhess-10-1851-2010

Melchiorre C, Matteucci M, Azzoni A, et al. (2008) Artificial neural networks and cluster analysis in landslide susceptibility zonation. Geomorphology 94: 379-400. DOI: 10.1016/j.geomorph.2006.10.035

Mohammady M, Pourghasemi HR, Pradhan B (2012) Landslide susceptibility mapping at Golestan Province, Iran: a comparison between frequency ratio, Dempster-Shafer, and weights-of-evidence models. Journal of Asian Earth Sciences 61: 221-236. DOI: 10.1016/j.jseaes.2012.10.005

Moore ID, Grayson RB (1991) Terrain-based catchment partitioning and runoff prediction using vector elevation data. Water Resources Research 27(6): 1171-1191. DOI: 10.1029/91WR00090

Muthu K, Petrou M, Tarantino C, et al. (2008) Landslide possibility mapping using fuzzy approaches. IEEE Transactions on Geoscience and Remote Sensing 46(4): 1253-1265. DOI: 10.1109/TGRS.2007.912441

Nefeslioglu HA, Sezer E, Gokceoglu C, et al. (2010) Assessment of Landslide Susceptibility by Decision Trees in the Metropolitan Area of Istanbul, Turkey. Mathematical Problems in Engineering 2010: 1-16. DOI: 10.1155/2010/901095.

Nefeslioğlu HA, Gokceoglu C, Sonmez H (2008) An assessment on the use of logistic regression and artificial neural networks with different sampling strategies for the preparation of landslide susceptibility maps. Engineering Geology 97(3/4): 171-191. DOI: 10.1016/j.enggeo.2008.01.004

Neuhäuser B, Terhorst B (2007) Landslide susceptibility assessment using "weights-of-evidence" applied to a study area at the Jurassic escarpment (SW-Germany). Geomorphology 86: 12-24. DOI: 10.1016/j.geomorph.2006.08.002

Oh HJ, Lee S (2011) Cross-application used to validate landslide susceptibility maps using a probabilistic model from Korea. Environmental Earth Sciences 64(2): 395-409. DOI: 10.1007/s12665-010-0864-0

Ozdemir A, Altural T (2013) A comparative study of frequency ratio, weights of evidence and logistic regression methods for landslide susceptibility mapping: Sultan Mountains, SW Turkey. Journal of Asian Earth Sciences 64: 180-197. DOI: 10.1016/j.jseaes.2012.12.014

Pachauri AK, Gupta PV, Chander R (1998). Landslide zoning in a part of the Garhwal Himalayas. Environmental Geology 36(3-4): 325-334. DOI: 10.1007/s002540050348

Pachauri AK, Pant M (1992) Landslide hazard mapping based on geological attributes. Engineering Geology 32: 81-100. DOI: 10.1016/0013-7952(92)90020-Y

Peng L, Niu R, Huang B, et al. (2014) Landslide susceptibility mapping based on rough set theory and support vector machines: A case of the Three Gorges area, China. Geomorphology 204: 287-301. DOI: 10.1016/j.geomorph.2013.08.013

Pellicani R, van Westen CJ, Spilotro G (2014) Assessing landslide exposure in areas with limited landslide information. Landslides 11(3):463-480. DOI: 10.1007/s10346-013-0386-4

Poudyal CP, Chang C, Oh H-J, et al. (2010) Landslide susceptibility maps comparing frequency ratio and artificial neural networks: a case study from the Nepal Himalaya. Environmental Earth Sciences 61: 1049-1064. DOI: 10.1007/s12665-009-0426-5

Pourghasemi HR, Moradi HR, Aghda SMF, et al. (2011) GIS based landslide susceptibility mapping with probabilistic likelihood ratio and spatial multi-criteria evaluation models (North of Tehran, Iran). Arabian Journal of Geosciences 7(5): 1857-1878. DOI: 10.1007/s12517-012-0825-x

Pourghasemi HR, Pradhan B, Gokceoglu C (2012) Application of fuzzy logic and analytical hierarchy process (AHP) to landslide susceptibility mapping at Haraz watershed, Iran. Natural Hazards 63(2): 965-996. DOI: 10.1007/s11069-012-0217-2

Pourghasemi HR, Pradhan B, Gokceoglu C, et al. (2013) A comparative assessment of prediction capabilities of Dempster-Shafer and Weights-of-evidence models in landslide susceptibility mapping using GIS. Geomatics, Natural Hazards and Risk 4(2): 93-118. DOI: 10.1080/19475705.2012.662915

Pradhan B, Lee S (2009) Landslide risk analysis using artificial neural network model focusing on different training sites. International Journal of Physical Science 4: 1-15.

Pradhan B (2010) Application of an advanced fuzzy logic model for landslide susceptibility analysis. International Journal of Computational Intelligence Systems 3: 370-381. DOI: 10.1080/18756891.2010.9727707

Pradhan B, Lee S (2010) Delineation of landslide hazard areas on Penang Island, Malaysia, by using frequency ratio, logistic regression, and artificial neural network models. Environmental Earth Sciences 60: 1037-1054. DOI: 10.1007/s12665-009-0245-8

Pradhan B (2011) Use of GIS-based fuzzy logic relations and its cross application to produce landslide susceptibility maps in three test areas in Malaysia. Environmental Earth Sciences 63(2): 329-349. DOI: 10.1007/s12665-010-0705-1

Pradhan B (2012) A comparative study on the predictive ability of the decision tree, support vector machine and neuro-fuzzy models in landslide susceptibility mapping using GIS. Computers & Geosciences 51: 350-365. DOI: 10.1016/j.cageo.2012.08.023

Rajbhandari PCL, Alam BM, Akther MS (2002) Application of GIS (Geographic Information System) for landslide hazard zonation and mapping disaster prone area: a study of Kulekhani Watershed, Nepal. Plan plus 1(1): 117-123.

Regmi AD, Yoshida K, Nagata H, et al. (2013) The relationship between geology and rock weathering on the rock instability along Mugling–Narayanghat road corridor, Central Nepal Himalaya. Natural Hazards 66(2): 501-532. DOI: 10.1007/s11069-012-0497-6

Regmi AD, Devkota KC, Yoshida K, et al. (2014) Application of frequency ratio, statistical index, and weights-of-evidence models and their comparison in landslide susceptibility mapping in Central Nepal Himalaya. Arabian Journal of Geosciences 7(2): 725-742. DOI: 10.1007/s12517-012-0807-z

Regmi NR, Giardino JR, Vitek JD (2010a) Assessing susceptibility to landslides: using models to understand observed changes in slopes. Geomorphology 112: 25-38. DOI: 10.1016/j.geomorph.2010.05.009

Regmi NR, Giardino JR, Vitek JD (2010b) Modeling

susceptibility to landslides using the weight of evidence approach: Western Colorado, USA. Geomorphology 115: 172-187. DOI: 10.1016/j.geomorph.2009.10.002

Roberts A (2001) Curvature attributes and their interpretation to 3D interpreted horizons: First Break 19: 85-100.

Shahabi H, Khezri S, Ahmad BB, et al. (2014) Landslide susceptibility mapping at central Zab basin, Iran: A comparison between analytical hierarchy process, frequency ratio and logistic regression models. Catena 115: 55-70. DOI: 10.1016/j.catena.2013.11.014

Santacana N, Baeza B, Corominas J, et al. (2003) AGIS-based multivariate statistical analysis for shallow landslide susceptibility mapping in La Pobla de Lillet Area (Eastern Pyrenees, Spain). Natural Hazards 30: 281-295. DOI: 10.1023/B:NHAZ.0000007169.28860.80

Searle MP, Windley B, Coward M, et al. (1987) The closing of Tethys and the tectonics of the Himalaya. Geological Society of America Bulletin 98: 678-701. DOI: 10.1130/0016-7606(1987)98<678:TCOTAT>2.0.CO;2

Sezer EA, Pradhan B, Gokceoglu C (2011) Manifestation of an adaptive neuro-fuzzy model on landslide susceptibility mapping: Klang valley, Malaysia. Expert Systems with Applications 38(7): 8208-8219. DOI: 10.1016/j.eswa.2010.12.167

Sharma M, Kumar R (2008) GIS-based landslide hazard zonation: a case study from the Parwanoo area, Lesser and Outer Himalaya, H.P., India. Bulletin of Engineering Geology and the Environment 67: 129-137. DOI: 10.1007/s10064-007-0113-2

Sidle RC, Pearce AJ, O'Loughlin CL (1985) Hillslope Stability and Land Use (Water Resources Monograph). American Geophys. Union, Washington, D.C., USA.

Soeters R, van Westen CJ (1996) Slope stability recognition analysis and zonation. In: Turner AK, Schuster RL (Eds.) Landslides: Investigation and Mitigation, Transportation Research Board Special Report 247. National Academy Press, Washington, D.C., USA. pp 129-177.

Tamrakar NK and Yokota S (2008) Types and processes of slope movements along East-West Highway, Surai Khola area, Mid-Western Nepal Sub-Himalaya. Bulletin of the Department of Geology, Tribhuvan University, Kathmandu, Nepal. 11: 1-4.

Umar Z, Pradhan B, Ahmad A, Jebur MN, Tehrany MS (2014) Earthquake induced landslide susceptibility mapping using an integrated ensemble frequency ratio and logistic regression models in West Sumatera Province, Indonesia. Catena 118: 124-135. DOI: 10.1016/j.catena.2014.02.005

Vahidnia MH, Alesheikh AA, Alimohammadi A, et al. (2010) A GIS-based neuro-fuzzy procedure for integrating knowledge and data in landslide susceptibility mapping. Computers & Geosciences 36(29): 1101-1114. DOI: 10.1016/j.cageo.2010.04.004

Van Westen CJ, Rengers N, Soeters R (2003) Use of geomorphological information in indirect landslide susceptibility assessment. Natural Hazards 30: 399-419. DOI: 1023/B:NHAZ.0000007097.42735.9e

Varnes DJ, International Association of Engineering Geology Commission on Landslides and Other Mass Movement on Slopes (1984) Landslides Hazard Zonation: A Review of Principles and Practice. Natural Hazards, Vol. 3. Published by UNESCO, Paris, France

Wu CH, Chen SC (2009) Determining landslide susceptibility in Central Taiwan from rainfall and six site factors using the analytical hierarchy process method. Geomorphology 112: 190-204. DOI: 10.1016/j.geomorph.2009.06.002

Yalcin A, Reis S, Aydinoglu AC, Yomralioglu T (2011) A GIS-based comparative study of frequency ratio, analytical hierarchy process, bivariate statistics and logistics regression methods for landslide susceptibility mapping in Trabzon, NE Turkey. Catena 85(3): 274-287. DOI: 10.1016/j.catena.2011.01.014

Yao X, Tham LG, Dai FC (2008) Landslide susceptibility mapping based on support vector machine: a case study on natural slopes of Hong Kong, China. Geomorphology 101(4): 572-582. DOI: 10.1016/j.geomorph.2008.02.011

Yesilnacar E, Topal T (2005) Landslide susceptibility mapping: a comparison of logistic regression and neural networks methods in a medium scale study, Hendek region (Turkey). Engineering Geology 79: 251-266. DOI: 10.1016/j.enggeo.2005.02.002

Yilmaz I (2009) Landslide susceptibility mapping using frequency ratio, logistic regression, artificial neural networks and their comparison: a case study from Kat landslides (Tokat-Turkey). Computers & Geosciences 35(6): 1125-1138. DOI: 10.1016/j.cageo.2008.08.007

Yoshimatsu H, Abe S (2006) A review of landslide hazards in Japan and assessment of their susceptibility using an analytical hierarchic process (AHP) method. Landslides 3: 149-158. DOI: 10.1007/s10346-005-0031-y

Zare M, Pourghasemi HR, Vafakhah M, et al. (2013) Landslide susceptibility mapping at Vaz watershed (Iran) using an artificial neural network model: a comparison between multi-layer perceptron (MLP) and radial basic function (RBF) algorithms. Arabian Journal of Geosciences 6(8): 2873-2888. DOI: 10.1007/s12517-012-0610-x

Zhu C, Wang X (2009) Landslide susceptibility mapping: a comparison of information and weights-of evidence methods in Three Gorges Area. International Conference on Environmental Science and Information Application Technology 3: 342-346.DOI: 10.1109/ESIAT.2009.187

Zhu A, Wang R, Qiao J, et al. (2014) An expert knowledge-based approach to landslide susceptibility mapping using GIS and fuzzy logic. Geomorphology 214: 128-138.